

UC Merced

UC Merced Previously Published Works

Title

Probabilistic Approach to Low Strain Rate Atomistic Simulations of Ultimate Tensile Strength of Polymer Crystals

Permalink

<https://escholarship.org/uc/item/25v7d9dc>

Journal

Journal of Chemical Theory and Computation, 19(18)

ISSN

1549-9618

Authors

Cobena-Reyes, José

Yang, Quanpeng

Stober, Spencer T

[et al.](#)

Publication Date

2023-09-26

DOI

10.1021/acs.jctc.3c00570

Copyright Information

This work is made available under the terms of a Creative Commons Attribution-NonCommercial-NoDerivatives License, available at

<https://creativecommons.org/licenses/by-nc-nd/4.0/>

Peer reviewed

Probabilistic approach to low strain rate atomistic simulations of ultimate tensile strength of polymer crystals

José Cobeña-Reyes,[†] Quanpeng Yang,^{†,‡} Spencer T. Stober,[¶] Adam B. Burns,[¶]
and Ashlie Martini^{*,†}

[†]*Department of Mechanical Engineering, University of California-Merced, 5200 N. Lake
Road, Merced, California 95343, United States*

[‡]*Department of Mechanical Engineering and Materials Science, Duke University, Durham,
North Carolina 27708, United States*

[¶]*ExxonMobil Technology and Engineering Company, 1545 Route 22 East, Annandale, New
Jersey 08801, United States*

E-mail: amartini@ucmerced.edu

Abstract

Molecular dynamics simulations of the tensile ultimate properties of polymer crystals require use of empirical potentials that model bond dissociation. However, fully reactive potentials are computationally expensive such that reactive simulations cannot reach the low strain rates of typical experiments. Here, we present a hybrid approach that uses the simplicity of a classical, non-reactive potential; information from bond dissociation energy calculations, and a probabilistic expression that mimics bond breaking. The approach is demonstrated for poly(*p*-phenylene terephthalamide) and, with one tunable parameter, the calculated tensile ultimate stress matches that obtained using a fully reactive simulation at high strain rates. Then, the hybrid simulations are run

at much lower strain rates where the ultimate tensile stress is strain rate independent and consistent with the expected experimental range.

Introduction

Crystalline polymers are important for various applications due to their combination of high strength and low weight. The prototypical example is poly(*p*-phenylene terephthalamide) (PPTA), which has very high ultimate tensile stress in the range of 2 to 5 GPa¹ with a low density between 1.45 and 1.5 g/cm³.^{2,3} However, research is still ongoing to further improve the tensile ultimate properties of PPTA⁴ or to combine it with other materials to create composites.⁵⁻⁷

Quantum mechanics and molecular modeling techniques, such as density functional theory (DFT) and molecular dynamics (MD) simulations, are important tools for understanding the tensile ultimate properties of polymer crystals. For instance, DFT has been used to study the role of the central N atom of the PPTA monomer in the strength of the polymer under compression⁸ and the relationship between inter-chain hydrogen bonds (H-bonds) and PPTA's ultimate tensile strength.⁹ MD simulations of PPTA have been conducted to study stress-strain behavior¹⁰⁻¹² and to model bond scission.^{10,13,14}

MD simulations that involve bond scission are of particular interest^{15,16} because they can be used to understand and possibly suggest ways to improve polymer strength.^{17,18} This type of simulation necessarily has a reactive force field that captures the breaking and formation of chemical bonds. The most common reactive force field for polymers is ReaxFF,¹⁹ which provides both accuracy and, in some cases, transferability.^{20,21} However, the number of equations, parameters, and correction terms in ReaxFF make it a computationally expensive model. Additionally, the typical time step for ReaxFF is between 0.05 and 0.5 fs, smaller than the 1-2 fs used in classical potentials for polymers such as OPLS,²² CHARMM,²³ and PCFF.²⁴ This limits ReaxFF simulations of polymer tensile ultimate properties to very high

strain rates, typically at least 10^8 s^{-1} .^{12,21}

To overcome this limitation, some attempts have been made to combine the simplicity of classical force fields with equations that model bond breaking. For example, the interface force field (IFF)²⁵ was modified to enable bond breaking²⁶ by replacing the harmonic bond energy term with the Morse potential equation.²⁷ Similarly, several other classical potentials have been modified with the Morse potential to enable bond breaking in stress-strain simulations, including modified versions of PCCF to model tensile failure of PPTA,²⁶ OPLS to model fracture in nanocomposites of silica and polybutadiene,²⁸ and the GAFF2^{29,30} potential to model the plastic properties of polymeric resins.³¹ Such hybrid approaches have speeds up to 50 times that of ReaxFF simulations and have been used to model polymer stress-strain behavior at strain rates as low as $2 \times 10^7 \text{ s}^{-1}$,²⁶ but are still several orders of magnitude higher than the strain rates accessible in experiments (in the range of $10^{-4} - 10^1 \text{ s}^{-1}$).^{1,32-35} As observed in our previous study,¹⁰ stress-strain behaviors of polyamides are highly strain rate dependent in simulations performed at such high strain rates. Thus, to faithfully reproduce stress-strain behaviors of polyamides, employing force fields that are fast and that can model bond scission in stress-strain simulations are highly desired.^{28,36}

Here, we present a modified simulation workflow for simulating tensile ultimate properties that uses the classical OPLS4³⁷ force field, and a probabilistic modification that uses  stretched exponential function based on the bond order equation from ReaxFF to model breaking of the weakest bond in the polymer. We employed MD simulations and DFT calculations to identify the weakest bond prior the simulations with OPLS4. Our results for PPTA show that, by using the OPLS4 force field with a modification that allows the weakest bonds in the polymer to break, it is possible to replicate the ultimate stress and strain from MD simulations modeled by ReaxFF at high strain rates. Additionally, we show that the hybrid simulation can be used for longer simulations and to calculate ultimate properties at orders of magnitude lower strain rates than accessible using ReaxFF that approach the magnitudes of experimentally reported values.

Models and Methods

Bond dissociation energy calculations

We created the PPTA monomer structure in Schrödinger³⁸ and computed the bond dissociation energy (BDE) of the four bonds identified in Fig. 1(a). The system was modeled at the M06-2X/6-311+G* level of theory,³⁹⁻⁴¹ which has been shown to be effective for aromatic amide polymers, such as PPTA.¹³ Here, we define the BDE as the difference in the standard enthalpy change between the whole molecule and the homolytically cleaved fragments.^{38,42}

Molecular dynamics simulations

A $6 \times 6 \times 6$ simulation cell of PPTA was built as shown in Fig. 1(b). The initial lattice parameters were obtained from Ref. 43. Two independent sets of simulations with two different force fields were performed: One set was modeled with ReaxFF⁴⁴ and the other with the OPLS4 potential.³⁷ The simulations using ReaxFF were run in LAMMPS⁴⁵ and the simulations with OPLS4 in Schrödinger.³⁸ All the cutoffs for ReaxFF were the default values in LAMMPS and for OPLS4 were the default value in Schrödinger. The time step size was 0.25 fs for the ReaxFF simulations and 1 fs for OPLS4. With both potentials, the model systems were minimized, and then equilibrated by running simulations in the NPT ensemble for 125 ps. In the ReaxFF simulations, the temperature and pressure were kept at 300 K and 1 atm by using the Nosé-Hoover thermostat and barostat with damping parameters of 10 fs and 100 fs, respectively. In the OPLS4 simulations, the Martyna-Tobias-Klein barostat and Nosé-Hoover thermostat were used with 2 ps and 1 ps damping parameters, respectively.

The density of the PPTA was averaged over the last 10 ps of the equilibration simulations and calculated to be $1.49 \pm 0.07 \text{ g/cm}^3$ with OPLS4 and $1.53 \pm 0.08 \text{ g/cm}^3$ with ReaxFF, both consistent with reported experimental results.^{2,3} Then, stress-strain deformation simulations were conducted in the NPT ensemble under ambient conditions in a step-wise manner, where the simulation boxes were stretched in the c-direction, along the

polymer backbone, by 0.25% and then relaxed for 2.5 ps to achieve an overall strain rate of $1 \times 10^9 \text{ s}^{-1}$. For each step, the stress of the systems was computed by averaging over the last 10% of time in the relaxation. This stretch-relax step was repeated until reaching 25% deformation or until failure. The results of simulations with both potentials were averaged over three independent simulations, each run with a different random seed number to create the initial atom velocity distribution. Additional simulations were run with OPLS4 using the same protocol at lower strain rates by straining the simulation box by a smaller amount in each step.

Modified classical potential for bond scission

The bond scission implementation in Schrödinger uses ~~the~~ stretched exponential function to compute the probabilities of the bonds being broken based on their length. In ReaxFF, the bond order is expressed as a sum of three exponential terms corresponding to the bond order contributions of σ , single π , and double π bonds, providing the flexibility to change the bond order during a reaction.¹⁹ However, if it is assumed that the bond order only decreases, as in a bond scission scheme, an equation involving only one exponential term should be sufficient for the bond order calculation. This assumption is the basis of the bond scission implementation in Schrödinger.³⁸

Bond types that are allowed to break are considered *reactive bonds*, and are specified in Schrödinger using a SMARTS⁴⁶ pattern. The probability of scission,  of each *reactive bond* is computed using the following stretched exponential equation:

$$P_i = \exp \left[-0.1 \left(\frac{l_i}{l_{eq}} \right)^9 \right] \quad (1)$$

The equilibrium length, l_{eq} , is the average of the lengths of the reactive bonds at the beginning of the simulation, and l_i is the length of each reactive bond computed at the end of each strain step i .³⁸ The constants -0.1 and 9 are ~~hard-coded in Schrödinger and~~ are related to

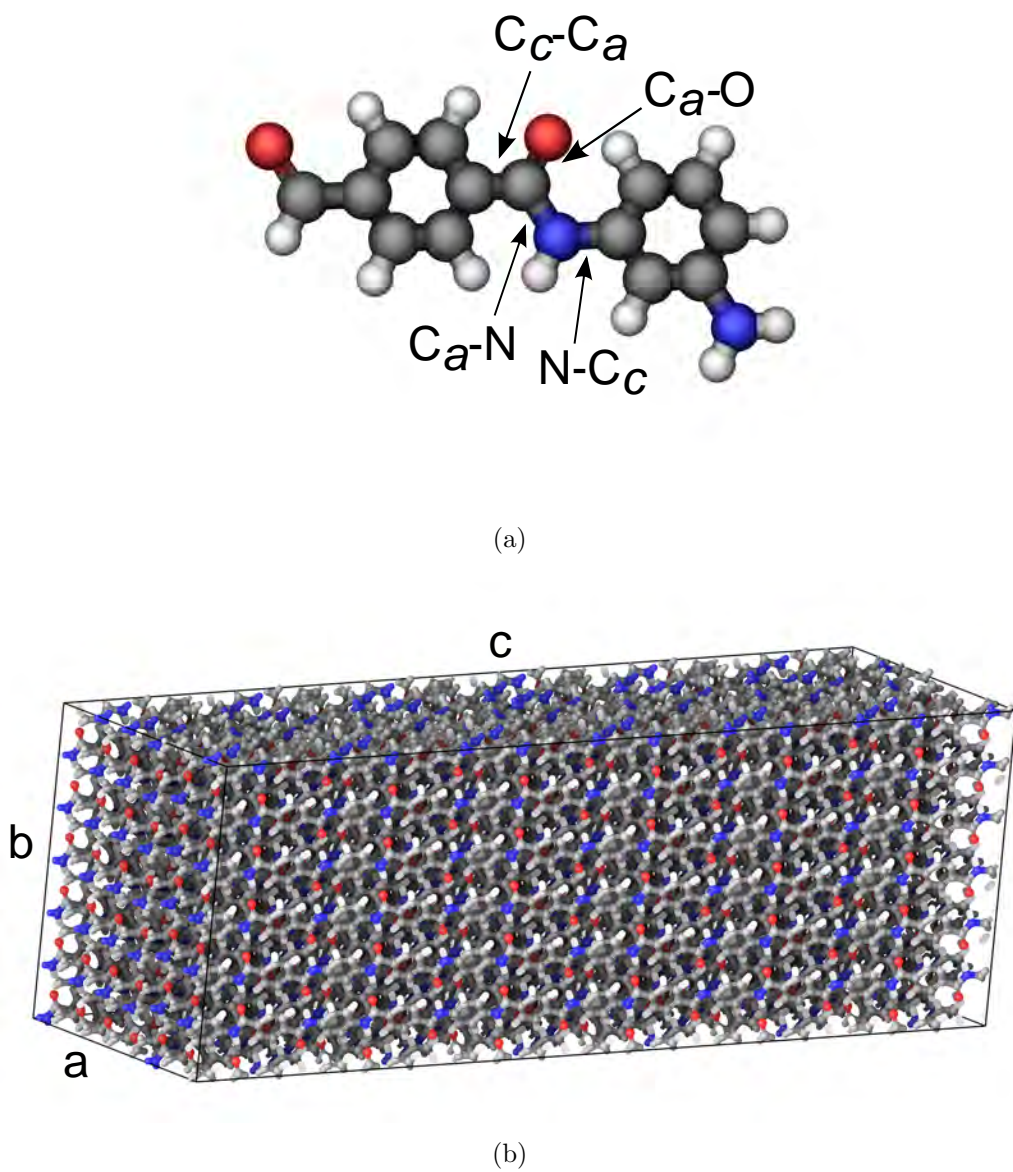


Figure 1: (a) PPTA monomer with the bonds evaluated in the bond dissociation calculation labeled. C_a and C_c correspond to aliphatic and cyclic carbon atoms, respectively. (b) $6 \times 6 \times 6$ PPTA simulation box after the NPT equilibration using OPLS4. The solid lines indicate periodic boundaries in all directions. Strain is applied in the c -direction. In both figures, C, H, O, and N atoms are represented by grey, white, red and blue spheres, respectively.

parameters in the [original ReaxFF implementation](#).

The *bond cutoff* is defined as the minimum percentage that a *reactive bond* must be elongated from l_{eq} to be a candidate for scission. The length associated with the *bond cutoff* is designed l_{bc} . The *bond cutoff probability*, P_{bc} , is also computed with Eq. 1, by replacing l_i

and P_i with l_{bc} and P_{bc} , respectively. Lastly, the *maximum bonds* is the maximum number of *reactive bonds* allowed to break. This parameter is set to 20, but its magnitude does not affect our results since the polymer was assumed to have failed after the first bond breaks based on the observation  that the first bond break corresponds to the drop in stress associated with failure. At each strain step, l_i and its probability P_i are computed. If $P_i > P_{bc}$, the bond i is not considered for scission; but if $P_i < P_{bc} \times R \sim \cup([0, 1])$, where R is a random number, then the bond is a candidate to be broken. If the number of candidate bonds is larger than *maximum bonds*, the bonds are selected randomly from the list of candidate bonds.

Results and discussion

The BDE results are presented in Table 1. The bond between the aliphatic C and the N, C_a -N, is the weakest, in agreement with previous results for PPTA from ReaxFF MD simulations^{13,14} and BDE calculations.⁸ The BDE of the other three bonds increases as C_c - $C_a < C_a$ -O $<$ N- C_c . This too is consistent with ReaxFF MD simulations that showed the C_c - C_a and C_a -N bonds are among the weakest in the PPTA monomer.¹¹

Table 1: Bond dissociation energies obtained using ~~M06-2X functionals and the 6-311G+*~~ basis set showing that C_a -N has the lowest BDE energy.

Bond	Bond energy [kcal/mol]
C_a -N	79.0
C_c - C_a	93.4
C_a -O	98.3
N- C_c	111.0

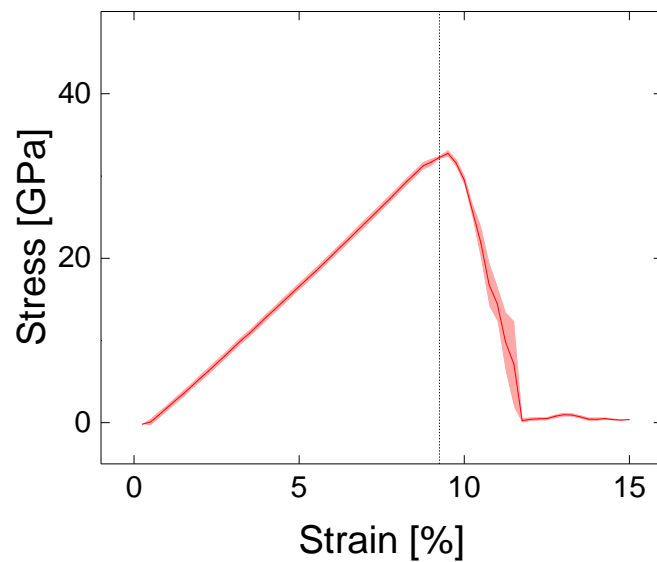
The stress-strain results from the ReaxFF simulation run at $1 \times 10^9 \text{ s}^{-1}$ are shown in Fig. 2a. The ultimate stress and strain are 32.7 GPa and 9.5%, respectively. This ultimate stress is much higher than experimental values, which are in the range of 2.7 – 3.4 GPa,^{1,33} but is consistent with previous ReaxFF MD simulations run at high strain rate.^{13,14} The failure is analyzed in terms of which bonds broke at each strain, as shown in Fig. 2b. The

first bond type that breaks is C_a-N, in agreement with our BDE results. The strain at which the C_a-N bonds start to break also corresponds to the onset of failure in the stress-strain plot. Therefore, this bond type is assigned as the *reactive bond* for the bond scission implementation in Schrödinger.

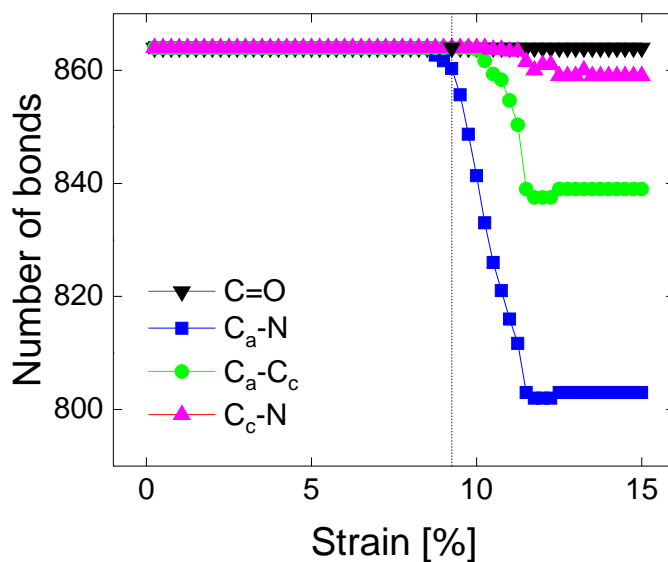
To obtain l_{bc} and the respective *bond cutoff*, we calculated the bond energy of the monomer using bond expansion simulations.¹¹ These simulations were run in the NVT ensemble at 300 K using the ReaxFF potential with the C_a-N bond length fixed at a values ranging from 1.2 to 2.0 Å. The simulations were run for 400 ps and the bond energy at each bond length was averaged over the last 100 ps. The energy vs. length data from the bond expansion simulations was fit to a polynomial to enable an analytical derivative to be taken. The stiffness of the bond was calculated as the second derivative of the fit bond energy expression.⁴⁷ The bond energy from ReaxFF (data and polynomial fit) and the second derivative of the fit are shown in Fig. 3. The bond length that corresponds to zero stiffness is 1.54 Å. The percentage difference between this length and the equilibrium length (1.45 Å) is 5.66%; this value is used as the *bond cutoff*.

We ran tension simulations in Schrödinger with the bond scission model using bond cutoff values between 4 and 12%. The ultimate stress and strain were calculated from each simulation from the point at which the first bond broke. The results are shown in Fig. 4. A bond cutoff of 5.66% gives ultimate stress consistent with that obtained from the ReaxFF simulation, shown as a red line in Fig. 4, indicating that the calculation of the bond cutoff based on the zero bond stiffness length is reasonable

To test the capability of our hybrid approach for modeling strain rates that approach experimental values, we used the same *bond cutoff* of 5.66% to run modified OPLS4 simulations at strain rates between 10⁵ and 10⁸ s⁻¹. The results are shown in Fig. 5. At high strain rates, the ultimate stress increases with strain rate, as seen in previous studies.^{33,48} Then, the results are approximately strain rate-independent for strain rates lower than about 10⁷ s⁻¹. This trend implies that 10⁷-10⁹ s⁻¹ is approximately the frequency of relaxation for the



(a)



(b)

Figure 2: (a) ReaxFF stress-strain results showing the polymer failed at a strain of 9.5%. The shaded area is standard deviation of three independent simulations. (b) Bond breaking profiles obtained during the strain simulation. The initial polymer failure corresponds to the breaking of C_a -N bonds. In both figures, a vertical black dashed line indicates 9.5% strain.

PPTA polymer.

For strain rates between 10^5 and 10^7 s^{-1} , the average simulated ultimate stress was 8.5

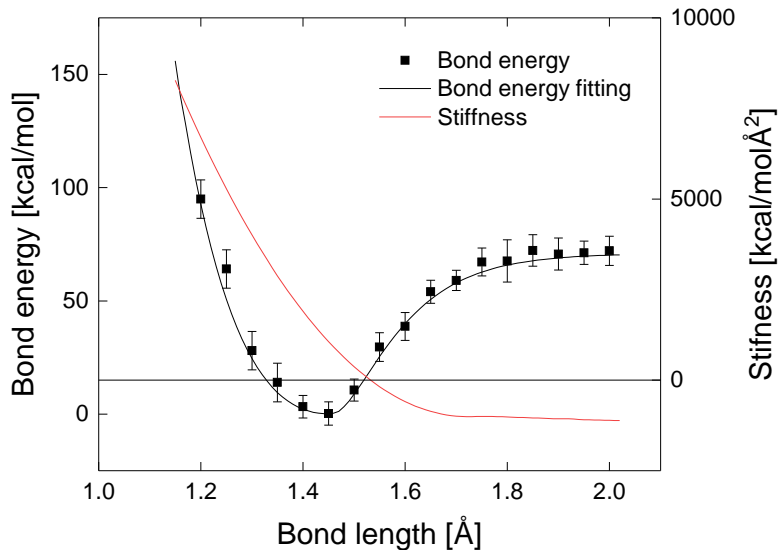


Figure 3: Bond energy and stiffness for the C_{α} -N bond from the ReaxFF potential. For bond energy, the symbols are calculated from bond expansion simulations and line is a polynomial fit to the data. Error bars reflect standard deviations of 4 independent simulations. The percent difference between the bond length at zero stiffness and the equilibrium length is the bond cutoff used to mimic bond scission with the OPLS4 potential.

GPa. This value is slightly lower than but on the same order of magnitude as experimental results measured at strain rates in the range of $10^{-4} - 10^{-3} \text{ s}^{-1}$.^{1,33-35} The difference between the experimental data and the low-strain simulation results is likely attributable to the ideal nature of the model PPTA. As mentioned in previous work,¹³ lack of defect nucleation sites and the presence of perfectly aligned infinite chains (due the presence of periodic boundary conditions) decrease the strength of the polymer. Regardless, these results show that our hybrid approach not only can mimic ReaxFF results at high strain rates, but also can approach experimental values at low strain rates when an appropriate bond cutoff is used.

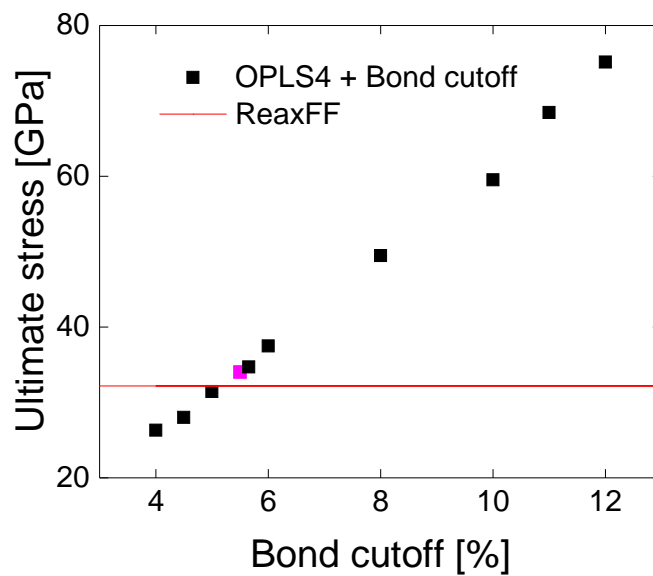


Figure 4: Ultimate tensile stress at a strain rate of 10^9 s^{-1} from ReaxFF (red line) and the modified OPLS4 with different values of the bond cutoff (black symbols). The minimum difference between ultimate stress from ReaxFF and OPLS4 is obtained with a bond cutoff of 5.66% (magenta square).

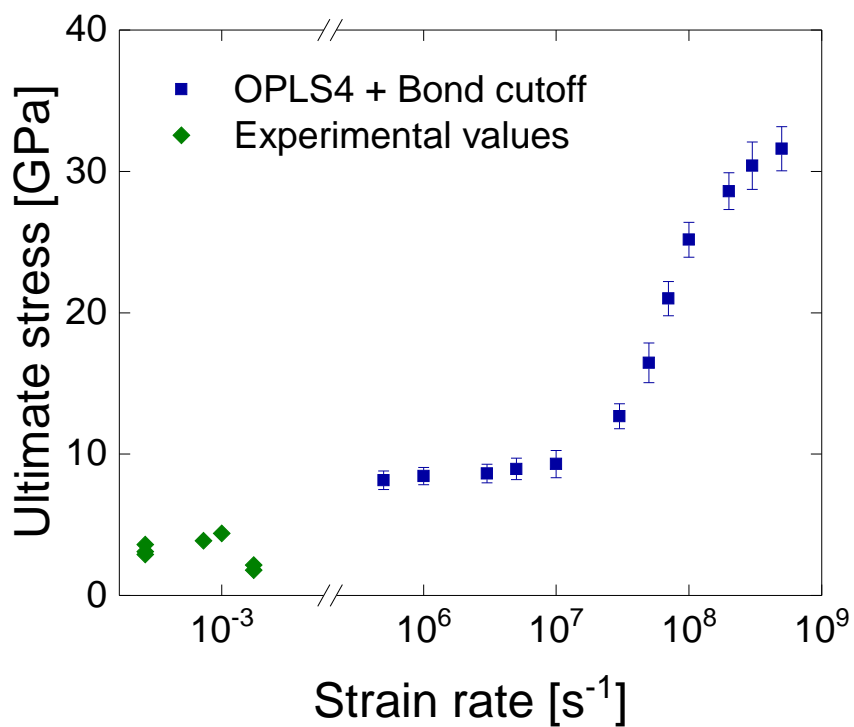


Figure 5: Ultimate stress vs strain rate calculated from simulations with OPLS4 and bond scission mimicked using a bond cut off of 5.66% (blue squares). Error bars are standard deviation of three independent simulations. Below 10^7 s^{-1} strain rate, the simulated ultimate stress is close to the reported experimental values (green diamonds).^{1,4,33–35,49}

Conclusions

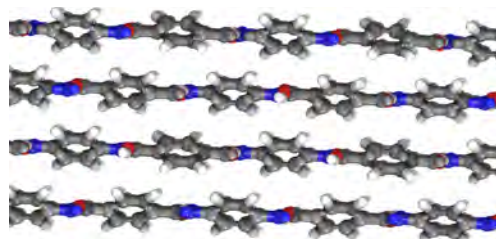
We presented a hybrid methodology to model stress-strain behavior and bond scission using MD simulations that employs the OPLS4 classical force field, bond dissociation energies computed from DFT simulations, and a probabilistic approach based on ReaxFF bond order equations. Simulations of tension of a PPTA crystal demonstrate that our methodology can provide similar ultimate stress to that obtained using ReaxFF. Additionally, we tested our method with strain rates approaching experimental values and the ultimate tensile stress obtained was on the same order of magnitude as that measured experimentally. We hope that this approach helps scientists accelerate their research towards a better understanding of the ultimate properties of polymer crystals and other high performance materials.

Acknowledgements

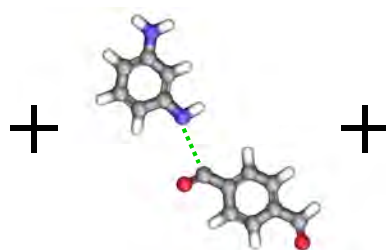
We thank Andrea Browning and Akin Budi for their help providing details of the bond scission probabilistic approach implemented in Schrödinger.

For Table of Contents Only

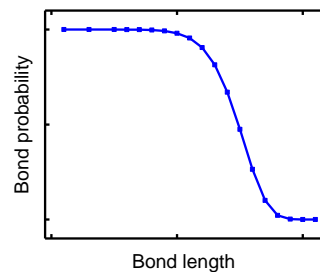
Classical molecular dynamics



Bond dissociation energy



Dissociation probability



References

- (1) Cline, J.; Wu, V.; Moy, P. *Assessment of the tensile properties for single fibers*; 2018; Report number: ARL-TR-8299.
- (2) Shim, V.; Lim, C.; Foo, K. Dynamic mechanical properties of fabric armour. *Int. J. Impact Eng.* **2001**, *25*, 1–15.
- (3) Yang, H. *Kevlar aramid fiber*; Wiley, 1993.
- (4) Rao, Y.; Waddon, A.; Farris, R. The evolution of structure and properties in poly (p-phenylene terephthalamide) fibers. *Polymer* **2001**, *42*, 5925–5935.
- (5) Xue, X.; Jiang, K.; Yin, Q.; Zhang, X.; Zhang, W.; Jia, H.; Ji, Q. Tailoring the structure of Kevlar nanofiber and its effects on the mechanical property and thermal stability of carboxylated acrylonitrile butadiene rubber. *J. Appl. Polym. Sci.* **2019**, *136*, 47698.
- (6) Dong, G.; Tang, Y.; Li, D.; Zhao, Y. F. Mechanical properties of continuous kevlar fiber reinforced composites fabricated by fused deposition modeling process. *Procedia Manuf.* **2018**, *26*, 774–781.
- (7) Lv, L.; Han, X.; Zong, L.; Li, M.; You, J.; Wu, X.; Li, C. Biomimetic hybridization of Kevlar into silk fibroin: nanofibrous strategy for improved mechanic properties of flexible composites and filtration membranes. *ACS nano* **2017**, *11*, 8178–8184.
- (8) Verma, H.; Rao, B. K.; Verma, M. L.; Chauhan, J. First principles study of breaking energy and mechanical strength of Kevlar-29. *Bull. Mater. Sci.* **2019**, *42*, 1–5.
- (9) Yu, J.; Fiorin, G.; Peng, H.; Klein, M. L.; Perdew, J. P. Different bonding type along each crystallographic axis: Computational study of poly (p-phenylene terephthalamide). *Phys. Rev. Mater.* **2020**, *4*, 055601.

- (10) Yang, Q.; Li, W.; Stober, S. T.; Burns, A. B.; Gopinadhan, M.; Martini, A. Molecular Dynamics Simulation of the Stress–Strain Behavior of Polyamide Crystals. *Macromolecules* **2021**, *54*, 8289–8302.
- (11) Yilmaz, D. E.; van Duin, A. C. Investigating structure property relations of poly (p-phenylene terephthalamide) fibers via reactive molecular dynamics simulations. *Polymer* **2018**, *154*, 172–181.
- (12) Chowdhury, S. C.; Gillespie Jr, J. W. A molecular dynamics study of the effects of hydrogen bonds on mechanical properties of Kevlar® crystal. *Comput. Mater. Sci.* **2018**, *148*, 286–300.
- (13) Yang, Q.; Li, W.; Stober, S. T.; Burns, A. B.; Gopinadhan, M.; Martini, A. Effect of Aliphatic Chain Length on the Stress–Strain Response of Semiaromatic Polyamide Crystals. *Macromolecules* **2022**, *55*, 5071–5079.
- (14) Mercer, B.; Zywickz, E.; Papadopoulos, P. Molecular dynamics modeling of PPTA crystallite mechanical properties in the presence of defects. *Polymer* **2017**, *114*, 329–347.
- (15) Liu, Q.; Liu, S.; Lv, Y.; Hu, P.; Huang, Y.; Kong, M.; Li, G. Atomic-scale insight into the pyrolysis of polycarbonate by ReaxFF-based reactive molecular dynamics simulation. *Fuel* **2021**, *287*, 119484.
- (16) Moller, J.; Barr, S.; Schultz, E.; Breitzman, T.; Berry, R. Simulation of fracture nucleation in cross-linked polymer networks. *JOM* **2013**, *65*, 147–167.
- (17) Zhang, Y.; Yuan, H.; Yan, W.; Zhang, Z.; Chen, S.; Liao, B.; Ouyang, X.; Chen, L.; Zhang, X. The effects of atomic oxygen and ion irradiation degradation on multipolymers: A combined ground-based exposure and ReaxFF-MD simulation. *Polym. Degrad. Stab.* **2022**, *205*, 110134.

- (18) Liu, X.; Li, X.; Liu, J.; Wang, Z.; Kong, B.; Gong, X.; Yang, X.; Lin, W.; Guo, L. Study of high density polyethylene (HDPE) pyrolysis with reactive molecular dynamics. *Polym. Degrad. Stab.* **2014**, *104*, 62–70.
- (19) Van Duin, A. C.; Dasgupta, S.; Lorant, F.; Goddard, W. A. ReaxFF: a reactive force field for hydrocarbons. *J. Phys. Chem. A* **2001**, *105*, 9396–9409.
- (20) Guo, W.; Fan, K.; Guo, G.; Wang, J. Atomic-scale insight into thermal decomposition behavior of polypropylene: A ReaxFF method. *Polym. Degrad. Stab.* **2022**, *202*, 110038.
- (21) Odegard, G. M.; Jensen, B. D.; Gowtham, S.; Wu, J.; He, J.; Zhang, Z. Predicting mechanical response of crosslinked epoxy using ReaxFF. *Chem. Phys. Lett.* **2014**, *591*, 175–178.
- (22) Jorgensen, W. L.; Maxwell, D. S.; Tirado-Rives, J. Development and testing of the OPLS all-atom force field on conformational energetics and properties of organic liquids. *J. Am. Chem. Soc.* **1996**, *118*, 11225–11236.
- (23) Brooks, B. R.; Brucoleri, R. E.; Olafson, B. D.; States, D. J.; Swaminathan, S. a.; Karplus, M. CHARMM: a program for macromolecular energy, minimization, and dynamics calculations. *J. Comput. Chem.* **1983**, *4*, 187–217.
- (24) Sun, H.; Mumby, S. J.; Maple, J. R.; Hagler, A. T. An ab initio CFF93 all-atom force field for polycarbonates. *J. Am. Chem. Soc.* **1994**, *116*, 2978–2987.
- (25) Heinz, H.; Lin, T.-J.; Kishore Mishra, R.; Emami, F. S. Thermodynamically consistent force fields for the assembly of inorganic, organic, and biological nanostructures: the INTERFACE force field. *Langmuir* **2013**, *29*, 1754–1765.
- (26) Winetrout, J. J.; Kanhaiya, K.; Sachdeva, G.; Pandey, R.; Damirchi, B.; van Duin, A.; Odegard, G.; Heinz, H. Implementing Reactivity in Molecular Dynamics Simulations

- with the Interface Force Field (IFF-R) and Other Harmonic Force Fields. *arXiv preprint arXiv:2107.14418* **2021**,
- (27) Morse, P. M. Diatomic molecules according to the wave mechanics. II. Vibrational levels. *Phys. Rev.* **1929**, *34*, 57.
- (28) David, A.; Tartaglino, U.; Casalegno, M.; Raos, G. Fracture in Silica/Butadiene Rubber: A Molecular Dynamics View of Design–Property Relationships. *ACS Polym. Au* **2021**, *1*, 175–186.
- (29) Wang, J.; Wang, W.; Kollman, P. A.; Case, D. A. Automatic atom type and bond type perception in molecular mechanical calculations. *J. Mol. Graph.* **2006**, *25*, 247–260.
- (30) Wang, J.; Wolf, R. M.; Caldwell, J. W.; Kollman, P. A.; Case, D. A. Development and testing of a general Amber force field. *J. Comput. Chem.* **2004**, *25*, 1157–1174.
- (31) Jang, C. W.; Mullinax, J. W.; Kang, J. H.; Palmieri, F. L.; Hudson, T. B.; Lawson, J. W. Microscopic deformation and failure modes of high-functionality epoxy resins from bond breaking molecular dynamics simulations and experimental investigation. *Polym. Eng. Sci.* **2022**, *62*, 3952–3963.
- (32) Utracki, L. *High Temperature Polymer Blends*; Elsevier, 2014; pp 14–69.
- (33) Zhu, D.; Mobasher, B.; Erni, J.; Bansal, S.; Rajan, S. Strain rate and gage length effects on tensile behavior of Kevlar 49 single yarn. *Composites, Part A* **2012**, *43*, 2021–2029.
- (34) Lim, J.; Zheng, J. Q.; Masters, K.; Chen, W. W. Effects of gage length, loading rates, and damage on the strength of PPTA fibers. *Int. J. Impact Eng.* **2011**, *38*, 219–227.
- (35) Cheng, M.; Chen, W.; Weerasooriya, T. Experimental investigation of the transverse mechanical properties of a single Kevlar® KM2 fiber. *Int. J. Solids Struct.* **2004**, *41*, 6215–6232.

- (36) Payal, R. S.; Fujimoto, K.; Jang, C.; Shinoda, W.; Takei, Y.; Shima, H.; Tsunoda, K.; Okazaki, S. Molecular mechanism of material deformation and failure in butadiene rubber: Insight from all-atom molecular dynamics simulation using a bond breaking potential model. *Polymer* **2019**, *170*, 113–119.
- (37) Lu, C.; Wu, C.; Ghoreishi, D.; Chen, W.; Wang, L.; Damm, W.; Ross, G. A.; Dahlgren, M. K.; Russell, E.; Von Bargen, C. D., et al. OPLS4: Improving force field accuracy on challenging regimes of chemical space. *J. Chem. Theory Comput.* **2021**, *17*, 4291–4300.
- (38) Bowers, K. J.; Chow, E.; Xu, H.; Dror, R. O.; Eastwood, M. P.; Gregersen, B. A.; Klepeis, J. L.; Kolossvary, I.; Moraes, M. A.; Sacerdoti, F. D., et al. Scalable algorithms for molecular dynamics simulations on commodity clusters. Proceedings of the 2006 ACM/IEEE Conference on Supercomputing. 2006; pp 84–es.
- (39) Zhao, Y.; Truhlar, D. G. Density functionals with broad applicability in chemistry. *Acc. Chem. Res.* **2008**, *41*, 157–167.
- (40) McLean, A.; Chandler, G. Contracted Gaussian basis sets for molecular calculations. I. Second row atoms, Z=11–18. *J. Chem. Phys* **1980**, *72*, 5639–5648.
- (41) Krishnan, R.; Binkley, J. S.; Seeger, R.; Pople, J. A. Self-consistent molecular orbital methods. XX. A basis set for correlated wave functions. *J. Chem. Phys.* **1980**, *72*, 650–654.
- (42) Bochevarov, A. D.; Harder, E.; Hughes, T. F.; Greenwood, J. R.; Braden, D. A.; Philipp, D. M.; Rinaldo, D.; Halls, M. D.; Zhang, J.; Friesner, R. A. Jaguar: A high-performance quantum chemistry software program with strengths in life and materials sciences. *Int. J. Quantum Chem.* **2013**, *113*, 2110–2142.
- (43) Deshmukh, Y. S.; Wilsens, C. H.; Verhoef, R.; Hansen, M. R.; Dudenko, D.; Graf, R.;

- Klop, E. A.; Rastogi, S. Conformational and structural changes with increasing methylene segment length in aromatic–aliphatic polyamides. *Macromol.* **2016**, *49*, 950–962.
- (44) Liu, L.; Liu, Y.; Zybin, S. V.; Sun, H.; Goddard III, W. A. ReaxFF-Ig: Correction of the ReaxFF reactive force field for London dispersion, with applications to the equations of state for energetic materials. *J.Phys. Chem. A* **2011**, *115*, 11016–11022.
- (45) Thompson, A. P.; Aktulga, H. M.; Berger, R.; Bolintineanu, D. S.; Brown, W. M.; Crozier, P. S.; in't Veld, P. J.; Kohlmeyer, A.; Moore, S. G.; Nguyen, T. D., et al. LAMMPS – a flexible simulation tool for particle-based materials modeling at the atomic, meso, and continuum scales. *Comput. Phys. Commun.* **2022**, *271*, 108171.
- (46) Daylight Chemical Information Systems, I. A language for describing molecular patterns. <https://www.daylight.com/dayhtml/doc/theory/theory.smarts.html>, (accessed October 2022).
- (47) Hybertsen, M. S. Modeling single molecule junction mechanics as a probe of interface bonding. *J. Chem. Phys.* **2017**, *146*, 092323.
- (48) Wang, Y.; Xia, Y. Experimental and theoretical study on the strain rate and temperature dependence of mechanical behaviour of Kevlar fibre. *Composites, Part A* **1999**, *30*, 1251–1257.
- (49) Dobb, M.; Johnson, D.; Saville, B. Compressional behaviour of Kevlar fibres. *Polymer* **1981**, *22*, 960–965.